Available online at www.sciencedirect.com

ScienceDirect

Procedia Structural Integrity 34 (2021) 59–64

Structural Integrity Procedia

www.elsevier.com/locate/procedia

The second European Conference on the Structural Integrity of Additively Manufactured Materials

The Effect of Printing Parameters on Crack Growth Rate of FDM ABS Cantilever Beam under Thermo-mechanical Loads

Feiyang He[a,*], Yousef Lafi A Alshammari[b], Muhammad Khan[c]

[a]*School of Aerospace, Transport and Manufacturing, Cranfield University, Bedford, MK43 0AL, UK*
[b]*School of Water, Energy and Environment, Cranfield University, Bedford, MK43 0AL, UK*
[c]*Centre for Life-cycle Engineering and Management, Cranfield University, Bedford, MK43 0AL, UK*

Abstract

Fused deposition modelling (FDM) is the most widely used additive manufacturing (AM) process in the customised and low-volume production industries. Acrylonitrile butadiene styrene (ABS) is the most commonly used thermoplastic printing material for FDM. The fabricated FDM ABS parts commonly work under thermo-mechanical loads in reality. In order to produce the high fatigue performance FDM ABS components, it is significant to investigate the effect of 3D printing parameters on crack growth. Hence, this research evaluated the crack propagation under bending fatigue test for FDM ABS beam in high-temperature conditions with varying printing parameters, including building orientations, nozzle size and layer thickness. The combination of three building orientations (0°, ±45° and 90°), three nozzle sizes (0.4, 0.6 and 0.8 mm) and three layer thickness (0.05, 0.1 and 0.15 mm) were tested under 50 to 70 °C environmental temperature ranges. The research attempted to investigate the relationship between crack growth rate and different printing parameter combinations. The study also attempted to determine the possible parameter combination which achieved the longest fatigue life for the FDM ABS specimen. Preliminary experimental results showed that the specimen with 0° building orientation, 0.8 mm filament width and 0.15 mm layer thickness vibrated for the longest time before the fracture at every different temperature.

© 2021 The Authors. Published by Elsevier B.V.
This is an open access article under the CC BY-NC-ND license (https://creativecommons.org/licenses/by-nc-nd/4.0)
Peer-review under responsibility of the scientific committee of the Esiam organisers

* Corresponding author. Tel.: +0044 7851975879.
E-mail address: Feiyang.he@cranfield.ac.uk

2452-3216 © 2021 The Authors. Published by Elsevier B.V.
This is an open access article under the CC BY-NC-ND license (https://creativecommons.org/licenses/by-nc-nd/4.0)
Peer-review under responsibility of the scientific committee of the Esiam organisers
10.1016/j.prostr.2021.12.009

Keywords: 3D printing; ABS; Crack growth rate; thermo-mechanical loads.

1. Introduction

Fused deposition modelling (FDM), as one of additive manufacturing technology, has been developed for about 30 years (Wang, Jiang, Zhou, Gou, & Hui, 2017). Due to its many advantages, such as safe, fast and efficient operation, freedom of customisation and cost-effectiveness, FDM is widely used in functional prototyping, aerospace, automotive and biomechanical fields (He, Kumar, & Khan, 2020).

There are several thermoplastic materials for FDM. Acrylonitrile butadiene styrene (ABS) is the most commonly used plastic because of its low expense, high strength, and temperature resistance (He & Khan, 2021). 3D-printed ABS products made from FDM can be used in extreme working environments (Espalin, Muse, MacDonald, & Wicker, 2014; Leigh, Bradley, Pursell, Billson, & Hutchins, 2012). Fatigue damage due to crack propagation is typical under these complex working conditions. The crack resistance and fatigue strength of the product are then significant and critical. However, only a handful of studies have evaluated the relationships between the printing parameters and crack propagation. Aliheidari et al. characterised the fracture resistance of FDM ABS specimens as a function of nozzle and bed temperatures. The research showed that the fracture resistance increased when the nozzle or bed temperature was increased (Aliheidari et al., 2017). Isaac and Tippur evaluated the effect of raster orientation on fracture behaviour for the FDM ABS specimen and revealed that the specimen with ±45° raster orientation has higher fracture toughness than 0/90° (Isaac & Tippur, 2019). Rabbi and Chalivendra investigated the effect of building orientation on fracture toughness for the FDM ABS specimen. The test results showed that dynamic fracture toughness was improved by 138% for a vertical printed specimen compared with a horizontal printed one (Rabbi, Chalivendra, & Li, 2019).

After reviewing previous research, only a few parameters have been evaluated for fracture behaviour of FDM ABS. Many key printing parameters have not yet been considered. Furthermore, no crack growth-related research considered the complex thermo-mechanical loads of the actual working environment. Therefore, this paper chose three critical printing parameters, including raster orientation, nozzle size and layer thickness, and investigated their influence on the crack growth rate of the FDM ABM cantilever beam under dynamic thermo-mechanical loads. The dynamic bending fatigue test was carried out. The obtained crack growth rate and stress intensity factor were used to develop the empirical crack growth model for the FDM ABS specimen.

Nomenclature

a	crack depth
A_i	the coefficient in governing motion equation of cantilever beam for ith cycle
a_i	initial crack depth
a_f	final crack depth$-acc_{i,trough}$
acc_i	acceleration in ith cycle
b	beam width
β_1	the coefficient for first mode vibration of the cantilever beam
C	coefficient in Paris Law
E_T	Temperature-dependant Young's Modulus
f_i	the fundamental frequency of beam in ith cycle
$f(a/H)$	a dimensionless boundary correction factor
H	beam thickness
I	second moment of area
ΔK	stress intensity factor range
l_c	distance from the fixed end of the beam to crack location
L	beam length
$M_i(l_c)$	the bending moment at the crack location in ith cycle
$\sigma_i(l_c)$	bending stress at the crack location in ith cycle
$\Delta\sigma$	stress range

T_i	period of ith cycle
$y_i(L)$	displacement amplitude at beam tip in ith cycle
$y_i(l_c)$	displacement amplitude at the crack location in ith cycle

2. Materials and specimen fabrication

The research chose a red ABS filament from Ultimaker® as the printing material. The raster orientation, nozzle size and layer thickness are investigated in the research. Three different values were chosen for each parameter, as listed in Table 1. There are 27 different parameter combinations for the values investigated in the research.

Table 1 Printing parameters

Raster orientation	Nozzle size (mm)	Layer thickness (mm)
0° (X)	0.4	0.05
±45° (XY)	0.6	0.10
90° (Y)	0.8	0.15

The only current standard for testing fatigue crack growth is ISO 12108. However, its limitations, such as the fact that it is only for metallic materials and only considers fatigue from cyclic mechanical loading, make it unsuitable for this study involving 3D printed polymers and thermo-mechanical loads. Therefore, for this research, we printed a specimen of the geometry shown in Figure 1.

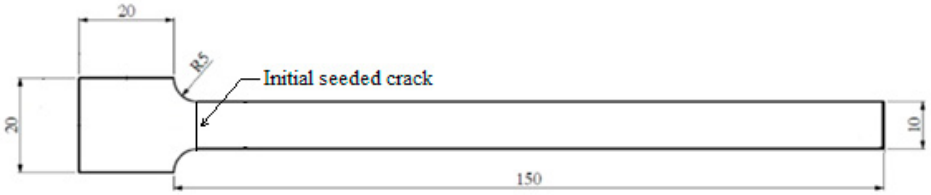


Figure 1 Geometry of specimen

The thickness of the specimen is 3 mm. An initial-seeded crack of 0.5 mm in depth was made close to the fixed end of the beam to ensure that the maximum stress concentration occurred at the exact location for all specimens.

3. Experimental details

Because the research introduced the thermal loads. 40, 50 and 60 °C, as different environmental temperatures, was applied in the test. Together with the printing parameters in Table 1, 81 combinations were tested in the research. Figure 2 shows the experimental setup, which is similar to previous work (Baqasah et al., 2019). The ABS specimen was fixed on the V55 shaker surrounded by a mica band heater providing the thermal loads. The signal generator and power amplifier provided the sinusoidal signal with 2mm amplitude to the shaker.

The specimens vibrated under fundamental frequency during the test. The maximum amplitude due to resonance significantly shortened the experiment time. The accelerometer at the beam tip recorded the acceleration data with crack propagation. The shaker's frequency also changed to keep the beam in resonance. The crack depth was measured by a Dino-Lite digital microscope during the test.

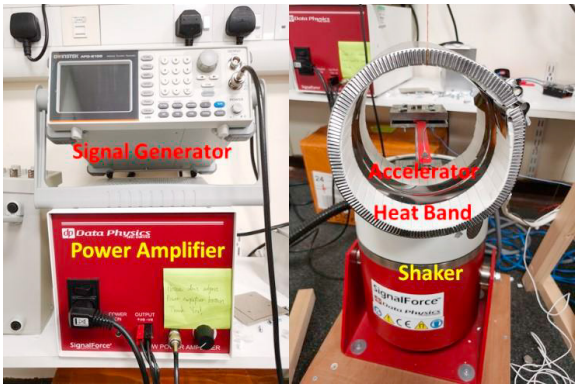


Figure 2 Experimental setup

4. Data process and crack growth rate model

4.1. Stress intensity factor (SIF) calculation

The SIF can be calculated by Eq.1 for mode I fracture in the test (Ostachowicz & Krawczuk, 1991). It is worth noting how to calculate the stress range $\Delta\sigma$ in the research. Unlike conventional fatigue crack growth tests, the stress range was time-variable due to varying beam amplitude during the test. An approximate calculation is essential. The average stress range was then calculated and substituted in Eq.1.

$$\Delta K = \Delta\sigma\sqrt{\pi a_i} f\left(\frac{a_i}{H}\right) \tag{1}$$

$$f\left(\frac{a}{H}\right) = 1.13 - 1.374\left(\frac{a}{H}\right) + 5.749\left(\frac{a}{H}\right)^2 - 4.464\left(\frac{a}{H}\right)^3$$

The mean stress amplitude at the crack location was calculated for each loading cycle by Eq.2 to Eq.7 step by step. As shown in Eq.2, the displacement amplitude at the crack tip was calculated by its quadratic integral relationship with acceleration amplitude measured by the accelerometer.

$$y_i(L) = \frac{1}{2}\frac{acc_{i,peak} - acc_{i,trough}}{(2\pi f_i)^2} \tag{2}$$

Then, the cracked beam was assumed as a full cantilever beam for simplifying calculations (Khan et al., 2015). The parameter in the governing motion equation for the cantilever beam under the vibration with fundamental frequency was calculated in Eq.3,

$$A_i = \frac{y_i(L)}{[\cos(\beta_1 L)+\cosh(\beta_1 L)] - \frac{\cos(\beta_1 L)-\cosh(\beta_1 L)}{\sin(\beta_1 L)-\sinh(\beta_1 L)}[\sin(\beta_1 L)+\sinh(\beta_1 L)]} \quad (\beta_1 L = 1.875104) \tag{3}$$

Therefore, the curvature and bending moment at the crack location can be calculated by Eq.4 and Eq.5,

$$\frac{d^2 y_i(l_c)}{dx^2} = A_i {\beta_1}^2 \left\{[-\cos(\beta_1 l_c) + \cosh(\beta_1 l_c)] - \frac{\cos(\beta_1 L)-\cosh(\beta_1 L)}{\sin(\beta_1 L)-\sinh(\beta_1 L)}[-\sin(\beta_1 l_c) + \sinh(\beta_1 l_c)]\right\} \tag{4}$$

$$M_i(l_c) = \left|E_T I \frac{d^2 y_i(l_c)}{dx^2}\right| \quad ; \quad I = \frac{bH^3}{12} \tag{5}$$

Then, assuming the bending stress at the crack tip was constant and equal to the stress on the beam surface, so

$$\sigma_i(l_c) = \frac{6M(l_c)}{bH^2} \tag{6}$$

Finally, because the beam vibrated up and down in the fatigue test, the single side crack was subjected to cyclic loading of tensile and compressive stresses. Moreover, only tensile stress contributed to the crack propagation. The stress range per cycle was introduced by the stress amplitude rather than the difference between peak and trough.

$$\Delta\sigma = \frac{\sum_{i=1}^{n} \sigma_i(l_c) T_i}{\sum_{i=1}^{n} T_i} \tag{7}$$

4.2. Crack growth rate calculation

As discussed in Section 4.1, the crack only propagated when the crack tip was under tensile loads. Therefore, the actual number of cycles is also half, so the mean crack growth rate between two crack depths is shown in Eq.8.

$$\frac{da}{dN} = 2\left(\frac{a_f - a_i}{N}\right) \quad (8)$$

4.3. Empirical model development

Paris law shown in Eq.9 can represent the relationship between crack growth rate and SIF range (Paris, Gomez, & Anderson, 1961). The study will determine the specific parameters for FDM ABS under different environmental temperatures. The SIF range and crack growth rate will be plotted. The curve fitting function in MATLAB will fit the data points and identify the suitable values for C and m.

$$\frac{da}{dN} = C(\Delta K)^m \quad (9)$$

5. Results and discussion

Specimens with different raster orientations, printed with the same 0.4 mm nozzle size and 0.05 mm layer thickness, were investigated preliminarily. The first-order polynomial curve fitting method was applied for log data. As a result, Figure 3 shows the crack growth rate change with different SIF for three raster orientations under 50 °C environmental temperatures. The fitted curves also determine the parameters of the Paris law, which is shown in Table 2.

All specimens show increased crack growth rate with increasing crack tip SIF. Specimen with X orientation had the lowest crack growth rate for the same stress intensity factor. The crack growth rate of the XY orientation specimen was between that of the X and Y orientation specimens. In contrast, the Y orientation specimen had the highest crack growth rate. This means that the X orientation specimens have the best fatigue strength and the Y orientation specimens have the shortest fatigue life for the same cyclic stress conditions.

The experimental results are similar to prior works, which fixed the loads frequency during crack propagation (He & Khan, 2021). It is reasonable. The initial seeded crack is lateral on the beam, which is Y raster orientation. Therefore, the 3D printing air voids in the Y orientation specimen has the same direction as the initial seeded crack. The presence of these printing defects between the filaments leads to stress concentration when the beam vibrates. It provides an excellent crack path that leads to quicker crack propagation. Also, the bonds between the fibres are the weakest in the areas where the voids are present. The occurrence of crazing is earlier in the area with the voids. Furthermore, the bending stress is longitudinal and acts vertically on the Y orientation voids during the beam's vibration. It accelerates the crack growth and decreasing fatigue life in the Y orientation specimen.

Table 2 Paris law constants determined by experimental data

Raster orientation	C	m	R-squared value
0° (X)	0.763	2.472*10E-4	0.9551
±45° (XY)	1.131	8.356*10E-3	0.9829
90° (Y)	0.8177	1.153*10E-3	0.8401

6. Conclusion and future works

This paper proposed an experimental method to investigate the printing parameters effect on the crack growth rate for FDM materials under thermo-mechanical loads. Preliminary experimental results showed that the specimens in X orientation have the lowest crack growth rates. The following study will compare the coefficients of the Paris law to evaluate the potential impact of different printing parameters on fracture behaviour. The study results will determine the optimal combination of printing parameters and guide future 3D printing setups.

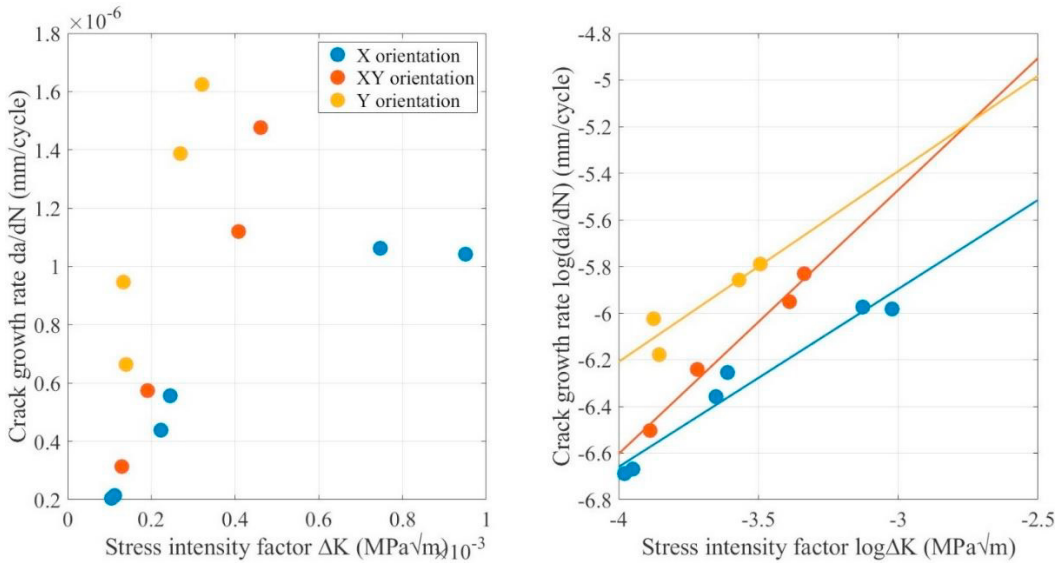


Figure 3 The crack growth rate of the specimens with different raster orientation, 0.05 mm layer thickness and 0.4 mm nozzle size under 50°C environmental temperature

References

Aliheidari, N., Tripuraneni, R., Hohimer, C., Christ, J., Ameli, A., & Nadimpalli, S. (2017). The impact of nozzle and bed temperatures on the fracture resistance of FDM printed materials. *Behavior and Mechanics of Multifunctional Materials and Composites 2017*, *10165*(April 2017), 1016512. https://doi.org/10.1117/12.2260105

Baqasah, H., He, F., Zai, B. A., Asif, M., Khan, K. A., Thakur, V. K., & Khan, M. A. (2019). In-situ dynamic response measurement for damage quantification of 3D printed ABS cantilever beam under thermomechanical load. *Polymers*, *11*(12). https://doi.org/10.3390/polym11122079

Espalin, D., Muse, D. W., MacDonald, E., & Wicker, R. B. (2014). 3D Printing multifunctionality: Structures with electronics. *International Journal of Advanced Manufacturing Technology*, *72*(5–8), 963–978. https://doi.org/10.1007/s00170-014-5717-7

He, F., & Khan, M. (2021). Effects of Printing Parameters on the Fatigue Behaviour of 3D-Printed ABS under Dynamic Thermo-Mechanical Loads. *Polymers*, *13*(14), 2362. https://doi.org/10.3390/polym13142362

He, F., Kumar, V., & Khan, M. A. (2020). Evolution and New Horizons in Modelling Crack Mechanics of Polymeric Structures. *Materials Today Chemistry*.

Isaac, J. P., & Tippur, H. V. (2019). Quasi-Static and Dynamic Fracture Behaviors of Additively Printed ABS Coupons Studied Using DIC : Role of Build Architecture and Loading Rate. In *Conference Proceedings of the Society for Experimental Mechanics Series* (Vol. 8, pp. 11–19).

Khan, M. A., Khan, S. Z., Sohail, W., Khan, H., Sohaib, M., & Nisar, S. (2015). Mechanical fatigue in aluminium at elevated temperature and remaining life prediction based on natural frequency evolution. *Fatigue and Fracture of Engineering Materials and Structures*, *38*(8), 897–903. https://doi.org/10.1111/ffe.12287

Leigh, S. J., Bradley, R. J., Purssell, C. P., Billson, D. R., & Hutchins, D. A. (2012). A Simple, Low-Cost Conductive Composite Material for 3D Printing of Electronic Sensors. *PLoS ONE*, *7*(11), 1–6. https://doi.org/10.1371/journal.pone.0049365

Ostachowicz, W. M., & Krawczuk, M. (1991). Analysis of the effect of cracks on the natural frequencies of a cantilever beam. *Journal of Sound and Vibration*, *150*(2), 191–201. https://doi.org/10.1016/0022-460X(91)90615-Q

Paris, P. C., Gomez, M. P., & Anderson, W. E. (1961). A rational analytic theory of fatigue. *The Trend in Engineering*, *13*, 9–14.

Rabbi, M. F., Chalivendra, V. B., & Li, D. (2019). A Novel Approach to Increase Dynamic Fracture Toughness of Additively Manufactured Polymer. *Experimental Mechanics*, *59*(6), 899–911. https://doi.org/10.1007/s11340-019-00486-3

Wang, X., Jiang, M., Zhou, Z., Gou, J., & Hui, D. (2017). 3D printing of polymer matrix composites: A review and prospective. *Composites Part B: Engineering*, *110*, 442–458. https://doi.org/10.1016/j.compositesb.2016.11.034



https://dspace.org/

The effect of printing parameters on crack growth rate of FDM ABS cantilever beam under thermo-mechanical loads

He, Feiyang; Alshammari, Yousef Lafi A.; Khan, Muhammad

2022-01-04
Elsevier
https://doi.org/10.1016/j.prostr.2021.12.009
He F, Alshammari YLA, Khan M. (2021) The effect of printing parameters on crack growth rate of FDM ABS cantilever beam under thermo-mechanical loads. Procedia Structural Integrity, Volume 34, 2021, pp. 59-64

Downloaded from a DSpace repository. https://dspace.org/